Murine norovirus abrogates *Chlamydia pneumoniae* accelerated atherosclerosis in ApoE$^{-/-}$ mice

Karuna Patil

A thesis
submitted in partial fulfillment of the
requirements for the degree of

Masters of Science
University of Washington
2015

Committee:
Charlie Hsu, VMD PhD DACLAM
Thea Brabb, DVM PhD DACLAM
Denny Liggitt, DVM PhD
Lee Ann Campbell, MS PhD

Program Authorized to Offer Degree:
Comparative Medicine

©Copyright 2015

Karuna Patil

University of Washington

Abstract

Murine norovirus abrogates Chlamydia pneumoniae accelerated atherosclerosis in ApoE$^{-/-}$ mice

Karuna Patil

Chair of the Supervisory Committee:

Charlie Hsu, VMD PhD DACLAM

Department of Comparative Medicine

*Chlamydia pneumonia*e (*Cpn*), a common respiratory pathogen of humans, has a strong seroepidemiologic association with cardiovascular disease as well as the ability to accelerate atherosclerosis in hyperlipidemic animal models. Our laboratory recently demonstrated that murine norovirus (MNV), a highly prevalent infection of laboratory mice, can variably alter atherosclerosis in hyperlipidemic Ldlr$^{-/-}$ and ApoE$^{-/-}$ mice. Given that MNV has a tropism for macrophages and has been shown to exacerbate atherogenesis under particular conditions, we investigated whether concurrent MNV and *Cpn* infection could alter macrophage phenotypes *in vitro* and atherosclerosis in ApoE$^{-/-}$ mice. In the presence of oxidized low-density lipoprotein (oxLDL), co-infection of ApoE$^{-/-}$ bone marrow derived macrophages (BMDM) with MNV and *Cpn* resulted in increases in gene expression of IL-6, MCP-1, iNOS, and TNF-α as compared with *Cpn* mono-infected BMDM. Based on these findings, we hypothesized that concurrent MNV infection would exacerbate vascular inflammation and increase plaque lesion size in *Cpn* infected ApoE$^{-/-}$ mice. As demonstrated previously, *Cpn* infection alone resulted in significantly

larger plaques (64% increase in mean size) as compared with uninfected mice. In mice co-infected with MNV and *Cpn* however, there was a 54% decrease in mean lesion size compared with *Cpn* mono-infected mice. Mechanisms by which MNV could elicit this unexpected abrogation in *Cpn* infected ApoE$^{-/-}$ mice were investigated. There were significant increases ($P < 0.05$) in the circulating Ly6C^{hi} monocyte subset in co-infected mice in comparison to either MNV mono-infected or uninfected mice. Further, there were no differences in cytokines locally at the site of lesion development, or in peritoneal macrophages 1 week following infection in mono-infected or co-infected mice as compared to controls. MNV was not detected in the aortic tissue of MNV infected mice at 1 week or 8 weeks post-infection regardless of *Cpn* status. These data suggest that MNV infection can abrogate the effect of *Cpn* on the progression of atherosclerosis and that this effect is likely through viral modulation of systemic responses rather than viral induction of inflammatory cytokines directly at the site of plaque formation in the aorta. These findings, regarding a highly prevalent virus of laboratory mice, should be a consideration for studies utilizing the ApoE$^{-/-}$ mouse model.

Dedication

This work is dedicated to my parents, brother, and all my teachers who have supported me through years of education and engendered my sense of curiosity.

Acknowledgements

This study was supported by the NIH grant R21-OD011135. I thank Jerry Ricks, Mark Berry, Gary Knowles, Nalini Agrawal, and Amy Lee for their technical assistance and Thea Brabb, Lillian Maggio-Price, Audrey Seamons, and Stacey Meeker for their support in the lab and critical evaluation of my work over the years. In addition I would like to acknowledge and thank the Chair of my Supervisory Committee, Charlie Hsu, for his relentless mentorship.

Table of Contents

Introduction

Cardiovascular disease (CVD) is the leading cause of mortality in the United States, accounting for nearly 37% of all deaths [42]. CVD refers to a number of conditions including atherosclerosis, the hardening and narrowing of arteries as a result of plaque buildup that can progress to myocardial infarction, stroke, and peripheral vascular disease. Atherosclerosis involves chronic vascular inflammation and while both genetic and environmental factors have been identified as risk factors, these alone do not completely account for all incidences of disease [11]. For this reason, much consideration has also been given to the role of infectious pathogens in atherosclerosis. Many pathogens, both viral and bacterial, have since been reported as having positive seroepidemiologic associations with atherosclerosis [11,36,37,44].

Chlamydia pneumoniae (*Cpn*), an obligate intracellular bacteria and prevalent respiratory pathogen in humans, is among the most studied agents implicated in contributing to atherosclerosis [1,5,6,23,30,36,37,44]. In addition to having a positive correlation between exposure to *Cpn* and CVD, this agent has been localized to and cultured from human atherosclerotic plaques [6,23]. Notably, the causality between the bacteria and disease has been demonstrated in animal models including hyperlipidemic rabbits, rats, and mice [1,5,6,15,30]. Viruses including cytomegalovirus, influenza A, and human immunodeficiency virus, have also been implicated in promoting vascular inflammation [2,3,16,28,44].

These infectious agents are thought to exert an effect on atherosclerosis through both direct and indirect mechanisms. Direct effects result from pathogen residence at the site of plaque formation. Localization of the pathogen can induce and worsen inflammation, cause dysfunction and proliferation of vascular cells, or alter lipid accumulation locally [36]. However, pathogens can also accelerate atherosclerosis without residence at sites of plaque formation via systemic effects [11,36]. Such indirect mechanisms include changes in circulating cytokine levels or in immune cell phenotypes [10,21,36,38].

Hyperlipidemic animal models have been useful tools in understanding the pathogenic mechanisms of these infectious agents in atherosclerosis [5,6]. Typically these animals are maintained “specific pathogen free”, meaning they are free of bacteria and viruses that are

known or suspected to interfere with research studies, but they may still be endemically infected with agents of unknown impact. Murine norovirus (MNV), a highly infectious and highly prevalent RNA virus is one endemic agent found in laboratory mice for which the impact of infection in mouse models of disease is still under investigation [13,35]. MNV infection is typically clinically silent in immunocompetent and even some immunocompromised hosts [13,41]. Initial *in vitro* studies with MNV revealed that the virus had a tropism for macrophages and dendritic cells [43]. For this reason, its potential effect on models of chronic inflammatory disease in which macrophages and dendritic cells play an important role including obesity, inflammatory bowel disease, and atherosclerosis has been investigated [17,18, 20,25,26,32,33,34].

Previously, our laboratory has shown that MNV infection in mouse models of atherosclerosis may alter plaque development but these effects may depend on genetics, timing of infection, or dietary fat content [17,32,34]. For example, MNV infection in $Ldlr^{-/-}$ mice promoted atherosclerotic lesion development and was associated with increased macrophage content [34], however this effect was dependent upon timing of infection [32]. Additionally, MNV infection increased atherosclerosis in $ApoE^{-/-}$ mice fed a standard chow diet, however this effect was variable [17]. Given the evidence from our laboratory that MNV may exacerbate atherosclerosis in hyperlipidemic mice, we chose to investigate both the possible direct and indirect effects of MNV in the $ApoE^{-/-}$ mouse model of *Cpn* accelerated atherosclerosis. We hypothesized that concurrent infection with MNV would alter macrophage and monocyte phenotypes, cytokine production, and ultimately result in larger atherosclerotic plaques in $ApoE^{-/-}$ mice as compared to animals infected with *Cpn* alone. We found however, while *Cpn* infection increased atherosclerotic plaque size as expected, concurrent infection with MNV resulted in decreased plaque size suggesting that MNV may in fact be atheroprotective in this model.

Methods

Bone marrow-derived macrophage infections. Bone marrow was harvested from ApoE$^{-/-}$ mice (9–12 weeks old) and differentiated as previously described [18]. Differentiated macrophages were plated at a density of 1 – 1.4 x 10^6 cells per well (6-well plates) in RPMI 1640 media containing 1% Nutridoma-SP (Roche, Indianapolis, IN), 1% penicillin–streptomycin, 20 μg/ mL gentamicin, and 10 μg/mL oxLDL with 4 treatment conditions: (1) uninfected, (2) MNV mono-infected, (3) *Cpn* mono-infected, and (4) MNV and *Cpn* co-infected. BMDM were inoculated with *Cpn* AR39 at a multiplicity of infection (MOI) of 5 in RPMI 1640 medium by centrifugation at 700 to 800 X g followed by 1 hour incubation at 37°C in 5% CO_2. *Cpn* containing media was removed and replaced with RPMI 1640 media described above. 24 hours after *Cpn* infection, cells were infected with MNV at a MOI of 0.2 or mock infected with clarified RAW 264.7 cell lysates free of MNV. Cells were harvested for RNA extraction using the RNeasy kit (Qiagen, Valencia, CA) 24 hours after MNV infection.

Animals. Male B6.129P2-*Apoe*^{tm1Unc}/J (ApoE$^{-/-}$) mice (6 weeks old) were purchased from the Jackson Laboratories (Bar Harbor, ME) and acclimated for 2 weeks prior to study. All mice were fed rodent chow (Picolab Rodent Diet 20 number 5053, PMI Nutrition, Brentwood, MO) and housed in individually ventilated cages (Thoren, Hazleton, PA) by infection status with corncob bedding (The Andersons, Maumee, OH). In addition, all had access to autoclaved, reverse osmosis, acidified water in bottles. Infectious agents excluded from the vivarium include mouse hepatitis virus, mouse parvovirus, minute virus of mice, reovirus-3, pneumonia virus of mice, epizootic diarrhea of infant mice, Theiler's murine encephalomyelitis virus, lymphocytic choriomeningitis virus, ectromelia virus, Sendai virus, sialodacryoadenitis virus, rat parvoviruses, *Mycoplasma pulmonis*, pinworms, and fur mites. MNV was excluded from the animal room except for experimental infections. Standard operating procedures employed to restrict MNV to experimentally infected mice were followed as previously described [33]. MNV infection status was confirmed prior to and at the end of each *in vivo* study via fecal RT-PCR [18]. All animal procedures were approved by the University of Washington's Institutional Animal Care and Use Committee**.**

Infections and tissue collection. Mice were assigned to one of four treatment groups: (1) uninfected control mice, (2) MNV mono-infected mice, (3) *Cpn* mono-infected mice, or (4) MNV and *Cpn* co-infected mice. For *Cpn* infections, 8-week-old ApoE$^{-/-}$ mice were intranasally dosed with *Cpn* strain AR39 resuspended in sucrose-phosphate-glutamic buffer. Mice were anesthetized with ketamine/xylazine and administered 3 x 10^7 inclusion forming units of *Cpn* in 20uL PBS or sham infected with 20uL sterile PBS as previously described [1,5]. This procedure was repeated at 9 and 10 weeks of age to establish a persistent infection. Two weeks later, mice were orally gavaged with 1 x 10^6 plaque forming units of MNV-4, passage 7, in 200 uL RAW 264.7 cell lysate or sham infected with clarified RAW 264.7 cell lysate free of MNV. Propagation and preparation of MNV-4 has been described previously [17,18].

To evaluate early changes associated with atherosclerosis development, ApoE$^{-/-}$ mice were euthanized with an inhaled overdose of CO_2 1 week after MNV infection (13 weeks old). Blood was collected by cardiac puncture and heparinized (20 units heparin per 1 mL blood) for flow cytometric analysis. Peritoneal macrophages were collected by a peritoneal lavage with 10 mL of sterile PBS, and cells were resuspended in RPMI 1640 media containing 10% FBS and 1% penicillin–streptomycin and incubated on 6-well plates for 1 hour at 37˚C. Following incubation, adherent cells (macrophages) were lysed and extracted for RNA using the RNeasy kit (Qiagen, Valencia, CA). The aortic arch was dissected free from surrounding adventitial tissue, and RNA was extracted using Lysing Matrix D tubes (MP Biomedical, Santa Ana, CA) and the RNeasy Fibrous Tissue Kit (Qiagen, Valencia, CA). A 2-3 mm portion of the descending thoracic aorta was collected and extracted using the Lysing Matrix D tubes and the RNeasy kit.

To evaluate changes in atherosclerotic plaque development, ApoE$^{-/-}$ mice were euthanized 8 weeks after MNV infection (20 weeks old). Mice were anesthetized with ketamine/xylazine and perfused with formalin after which the heart was collected and stored in formalin. A 2-3mm portion of the descending thoracic aorta was stored in RNAlater (Ambion, Austin, TX) and frozen at -80˚C.

Real-time RT-PCR. RNA from both BMDM and tissue samples was converted to cDNA using the SuperScript First Strand Synthesis System (Invitrogen). Real time RT-PCR was performed with the Power SYBR Green Master Mix (Applied Biosystems) and a Stratagene Mx3005P analyzer (Agilent Technologies). Primer sequences utilized for various genes were previously described [9,12,14,18,22,27,29]. Target gene expression in aortic arch samples was normalized to β-actin and expressed as a fold change relative to a control sample (RNA from aortic tissue of an uninfected mouse) that was run on every plate as a calibrator. Target gene expression for peritoneal macrophages and BMDM was normalized to the housekeeping gene hypoxanthine-guanine phosphoribosyltransferase (HPRT) and presented as the fold change relative to the average value obtained from uninfected animals or uninfected cells.

Quantification of atherosclerosis. Quantification of plaque size from 20-week-old ApoE$^{-/-}$ mice was performed as previously described utilizing Movat's Pentachrome stain and scored by a researcher blinded to treatment groups [32,34].

Flow cytometric analysis of peripheral blood. Red blood cells were lysed in heparinized blood using Gey's solution, cell count was determined, and samples were blocked with anti-CD16/CD32 antibody (BD Biosciences, San Jose, CA). Anti-mouse antibodies were then used to label cell surface markers including Lineage (Lin) (NK1.1, CD90.2, B220, Ly6G, Ter119, and CD49b), Ly6C, CD11b, CD11c, I-A/I-E, and F4/80 (all obtained from BD Biosciences). Leukocytes were gated on FSC-A and SSC-A and single cells were gated on FSC-A and FSC-W parameters. Lin- cells were further gated to identify monocytes (Lin-CD11b+F4/80-Class II-CD11c-). Monocytes were also characterized based on Ly6C expression. Samples with less than 80 events in the monocyte gate were excluded from analysis (low number artifact). Data was collected on a BD LSRII and analyzed using FlowJo (Tree Star, Inc., Ashland, OR).

RT-PCR for MNV-4 detection. RT-PCR for detection of MNV-4 was performed using primers as previously described [18] in the aortic arch and descending aorta samples from 13-week-old ApoE$^{-/-}$ mice, and descending aorta samples from 20-week-old ApoE$^{-/-}$ mice of various infection status.

Statistics. Data was analyzed using Prism statistical software (GraphPad Software, La Jolla, CA). One-way ANOVA with post hoc test (Tukey's Multiple Comparison) was used for comparison between 4 groups, whereas a *t* test was used for comparison of 2 groups.

Results

MNV increases gene expression of IL-6 and MCP-1 in *Cpn* infected ApoE$^{-/-}$ BMDM.

To evaluate the effect of MNV and *Cpn* on macrophage activation and recruitment, ApoE$^{-/-}$ BMDM were infected in the presence of oxLDL with MNV alone, *Cpn* alone, or both agents combined and gene expression for IL-6, IL-1β , and MCP-1 were evaluated. Infections were performed in the presence of oxLDL to better mimic the *in vivo* plaque environment which is rich in lipids. *Cpn* mono-infection increased IL-6, IL-1β and MCP-1 expression compared to uninfected and MNV mono-infected BMDM (Figure 1). Co-infection with MNV and *Cpn* led to further increases in IL-6 and MCP-1 but not IL-1β expression as compared with *Cpn* mono-infected cells (Figure 1). These data suggest that MNV infection can enhance IL-6 and MCP-1 gene expression in ApoE$^{-/-}$ BMDM already infected with *Cpn*.

MNV exacerbates a pro-inflammatory macrophage phenotype in *Cpn* infected ApoE$^{-/-}$ BMDM.

To evaluate the effect of MNV and *Cpn* on macrophage phenotype, gene expression for markers of classically activated macrophages (M1: iNOS, IL-12β, TNF-α) as well as alternatively activated macrophages (M2: Arg1, IL-10) were measured. M1 and M2 phenotypes, which have both been demonstrated in atherosclerotic plaques, have opposing functions in that M1 macrophages promote inflammation while M2 macrophages are regulatory and help to dampen and control local inflammatory responses [10,21,24].

Cpn infection alone significantly increased IL-12β by 700 fold, TNF-α by 10 fold, and iNOS by 14,000 fold as compared to the uninfected control (Figure 2A). Co-infected BMDM displayed a 4 fold increase in iNOS and a 13 fold increase in TNF-α gene expression as compared with *Cpn* mono-infected cells. IL-12β expression was increased in co-infected cells with a mean fold change of 867 compared with a mean increase of 695 fold in *Cpn* mono-infected animals. MNV infection alone induced more moderate increases in iNOS, IL-12β, and TNF-α. *Cpn* mono-infection also elicited an M2 response with increases in the expression of Arg1 and IL-10 as compared to uninfected BMDM (Figure 2B). Co-infection dampened this M2 response indicated by a decrease in the relative expression of Arg1 as compared with *Cpn* mono-infected mice.

MNV mono-infection had a lesser effect on M2-associated genes, with smaller increases in Arg1 and IL-10 as compared with the effect of *Cpn* mono-infection (Figure 2B). These findings suggest that *Cpn* can elicit an M1 pro-inflammatory macrophage phenotype that is exacerbated by concurrent MNV infection. In addition there is evidence that while *Cpn* mono-infection elicits an M2 phenotype, co-infection attenuates this regulatory M2 macrophages response.

MNV infection abrogates *Cpn* accelerated atherosclerosis in ApoE$^{-/-}$ mice.

Given our *in vitro* findings that MNV increased MCP-1 and IL-6 expression, as well as exacerbated the pro-inflammatory macrophage phenotype in *Cpn* infected ApoE$^{-/-}$ BMDM, we hypothesized that concurrent infection with MNV would result in exacerbation of *Cpn* accelerated atherosclerosis. To test this, ApoE$^{-/-}$ mice of various infection status (no infection, MNV only, *Cpn* only, and co-infection) were examined at 20 weeks of age (12 weeks following *Cpn* infection, 8 weeks following MNV infection) for atherosclerotic lesion size in the aortic sinus. Infection with *Cpn* significantly increased (P = 0.04) the average aortic sinus lesion area (34648 ± 5015 μm^2) by approximately 62% when compared to uninfected controls (21443 ± 2305 μm^2) (Figure 3). Unexpectedly, co-infected animals had smaller plaque lesion size as compared with *Cpn* mono-infected animals. A 56% reduction in the average aortic lesion area (22800 ± 3004 μm^2) was observed in co-infected animals as compared with *Cpn* mono-infected animals although this difference did not reach statistical significance (P = 0.057). MNV mono-infection did not increase plaque lesion size compared to uninfected controls. Taken together, these data suggest that MNV infection abrogated the effect of *Cpn* on atherosclerosis in this hyperlipidemic animal model.

MNV alters circulating monocyte populations in *Cpn* infected ApoE$^{-/-}$ mice.

One proposed indirect mechanism by which pathogens alter lesion size is through an effect on circulating monocytes. Monocytes differ in their recruitment to and function within the plaque [38,40]. Murine monocytes can be differentiated by their Ly6C surface expression and it has been shown that Ly6C^{hi} monocytes are preferentially recruited to plaques where they differentiate into pro-inflammatory macrophages [10,39]. In order to determine whether MNV infection could lead to alterations in circulating monocytes of *Cpn* infected animals which could

account for our *in vivo* findings, peripheral blood from 13-week-old ApoE$^{-/-}$ mice was evaluated in uninfected, MNV mono-infected, *Cpn* mono-infected, and co-infected mice. No differences were noted in the percent monocytes in peripheral blood (Figure 4A). Further, while there were no differences in percent Ly6C^{hi} monocytes of *Cpn* mono-infected mice, there was a significant increase in the percentage of Ly6C^{hi} monocytes in mice co-infected with both MNV and *Cpn* (10.6% ± 3.7%) relative to uninfected mice (1.1% ± 0.3%) (Figure 4B). The percentage of Ly6C^{hi} monocytes was also significantly different between co-infected animals and MNV mono-infected mice (2.3% ± 1.1%). These findings suggest that while neither infection results in alterations in monocyte numbers, co-infection with MNV and *Cpn* does result in a phenotypic shift towards increased Ly6C^{hi} monocytes.

No alterations in cytokine, chemokine, or adhesion molecule expression at the site of lesion development in the aorta, or in peritoneal macrophages.

In order to determine whether cytokines were directly altered in the local environment of plaque development in the aorta, gene expression in the aortic arch of 13-week-old ApoE$^{-/-}$ mice of various infection status (no infection, MNV only, *Cpn* only, and co-infection) was evaluated. In addition to looking directly at the site of lesion formation, gene expression of peritoneal macrophages from these mice was assessed since they have the potential to influence lesion development indirectly if recruited into developing plaques. No significant differences were detected in aortic arch MCP-1, TNF-α, or IL-1β expression between any of the infection groups (Figure 5A). Likewise, no differences in gene expression of MCP-1, TNF-α, or Arg1 were seen in peritoneal macrophages (Figure 5B). Further, given that we observed a robust increase in iNOS expression following *in vitro* co-infection of BMDM with MNV and *Cpn* (Figure 2A) we evaluated iNOS expression in the aortic arch and found no differences between any groups (data not shown).

Adhesion molecules can also contribute significantly to atherogenesis because they, in part, regulate the rate and number of monocytes and macrophages entering developing lesions [10]. To this effect, we examined expression of ICAM-1 in the aortic arch tissue where MNV may exert a direct effect, as well as in peritoneal macrophages which if altered following infection

could influence lesion development indirectly. There were no significant differences in relative expression of ICAM-1 among infection groups in either the aortic arch or in peritoneal macrophages (Figure 6).

MNV is not detectable in aortic tissue of infected ApoE$^{-/-}$ mice.

In order to determine whether MNV localizes to sites of atherosclerosis in ApoE$^{-/-}$ mice acutely following infection and during the early lesion development process, RT-PCR for MNV was performed on the aortic arch and descending aorta tissue 1 week following MNV infection in 13-week-old ApoE$^{-/-}$ mice. MNV was not detected in the aortic tissue of any of the mice regardless of *Cpn* status. To determine whether MNV localizes to the site of lesion development during chronic stages of atherosclerosis, RT-PCR for MNV was also performed on the descending aorta of 20-week-old mice, 8 weeks after MNV infection. Similarly, MNV was not detected in any mice regardless of *Cpn* status. In order to confirm that animals gavaged with MNV were infected, MNV RT-PCR was performed on pooled feces from each mouse cage. All fecal samples from cages of mice experimentally infected with MNV were positive by MNV RT-PCR at both 1 and 8 weeks post-infection while feces from uninfected cages were confirmed negative.

Discussion

Atherosclerosis is a leading cause of morbidity in humans and involves chronic systemic vascular inflammation. The innate immune system is a major contributor to this process and macrophages and monocytes are key components of atherosclerotic plaques [10,11,24,38]. Local and/or systemic changes in these cells, such as those that occur in response to infection, are thought to underlie pathogen accelerated atherosclerosis. Considerable evidence in humans, as well as in animal studies has implicated the common respiratory pathogen *C. pneumoniae* as a risk factor for cardiovascular disease. Hyperlipidemic animal models have been utilized to understand how this pathogen may augment atherogenesis and *Cpn* infection in ApoE$^{-/-}$ mice has been reported to increase atherosclerotic plaque lesions size [2,5,30]. Our laboratory has previously demonstrated that MNV, an endemic viral infection of laboratory mice, variably alters atherosclerosis in both Ldlr$^{-/-}$ and ApoE$^{-/-}$ mouse models [17,32,33]. Given the potential of this virus to interfere with atherosclerosis, we investigated the effect of MNV and *Cpn* co-infection in ApoE$^{-/-}$ mice and hypothesized that co-infection would lead to increase expression of inflammatory cytokines and chemokines, and exacerbate atherosclerotic lesion size as compared to *Cpn* mono-infection.

Co-infection of BMDM exposed to oxLDL, used to mimic the hyperlipidemic environment in which plaques form *in vivo*, resulted in significant increases in gene expression of IL-6 and MCP-1 in addition to eliciting an M1 pro-inflammatory macrophage phenotype evidenced by increases in iNOS and TNF-α. Although macrophages within vascular tissue have not been specifically studied, our *in vitro* BMDM findings are in agreement with studies demonstrating that *Cpn* induces M1 macrophages following pulmonary infection [19]. IL-6 and MCP-1 are strong macrophage chemoattractants and have been correlated with increased plaque macrophage content [10,24] while iNOS and TNF-α are potent pro-inflammatory factors that contribute to sustained vascular inflammation [11]. Macrophage subtypes have been shown to play differing roles in plaque development [10,21,24]. Classically activated macrophages (M1, characterized by iNOS, IL-12β, TNF-α) contribute to sustained inflammation whereas alternatively activated macrophages (M2, characterized by Arg1 and IL-10) appear to stabilize

the plaque [9,12,21,24]. These *in vitro* findings suggest that MNV may exacerbate *Cpn* accelerated atherosclerosis in ApoE$^{-/-}$ mice through changes in either circulating or plaque resident macrophages.

The inability to detect MNV in aortic tissues of infected animals either 1 or 8 weeks post infection favors the explanation that MNV would have an indirect effect on atherogenesis. A recent publication demonstrated that atherosclerotic lesions in ApoE$^{-/-}$ mice were proportional to intra-lesional monocyte accumulation [40] suggesting that an effect on monocytes in particular would result in significant changes to plaque development. Further a subset of these cells, Ly6C^{hi} monocytes, have been shown to both preferentially adhere to inflamed endothelium and give rise to pro-inflammatory macrophages [37]. Here we show that while MNV does not affect percent blood monocytes 1 week after infection with MNV, co-infected animals have an increase in the Ly6C^{hi} subset suggesting that plaque lesion size in co-infected animals would also be increased after co-infection.

In our study, while infection with *Cpn* significantly increased the average aortic sinus lesion area by 62% compared to uninfected controls as expected and reported by others [2,5,30], concurrent infection with MNV unexpectedly resulted in a decrease in lesion size. In general, this is in disagreement with studies in humans that have found a positive correlation between the number of infections experienced by a patient (infectious burden) and cardiovascular disease [37,44]. Further, this is in disagreement with our *in vitro* data of increased pro-inflammatory cytokines and macrophages, and our analysis of circulating Ly6C^{hi} monocytes which were increased following co-infection. One explanation may be that perhaps BMDM are not predictive of atherosclerosis *in vivo*, and that the disagreement between our *in vitro* and *in vivo* findings may be due to the complexity of downstream effects of the chemokines and cytokines evaluated. For example, while iNOS is typically thought of as pro-inflammatory, it has also been shown to be atheroprotective against *Cpn* accelerated disease [7]. Another explanation may be that monocyte populations are responsive to many systemic factors [38,39] and so may change over time. Our finding of increased Ly6C^{hi} monocytes at 1 week post MNV infection may have been transient or could have been subsequently altered by systemic

responses. Further mechanistic work is needed to understand how MNV decreased plaque size *in vivo.*

There is emerging evidence that resident viruses help define immunophenotype, systemic inflammation and even disease susceptibility [4,8]. While members of the genus *Norovirus* are traditionally thought of as pathogenic [13], our *in vivo* findings suggest that this particular norovirus may be atheroprotective. Our *in vivo* finding is similar to a study in which ApoE$^{-/-}$ mice were co-infected with murine cytomegalovirus and *Cpn*: while *Cpn* led to significant increases in lesion size, concurrent infection with cytomegalovirus abrogated this effect demonstrating viral protection against *Cpn* accelerated atherosclerosis [2]. Our findings are also consistent with a recent study in which MNV conferred protection to antibiotic treated mice against pathogenic bacterial challenge with *Citrobacter rodentium* [19]. Mice infected with MNV prior to *C. rodentium* challenge had reduced weight loss, diarrhea, and intestinal injury supporting the notion that under certain conditions MNV may be protective [19].

Taken together these data suggest that consideration should be given to how viral infections such as MNV can alter disease phenotype since endemic viruses may be intercurrent variables. Further, due to the high prevalence of MNV and the atheroprotective effects in the *Cpn* accelerated ApoE$^{-/-}$ model reported herein, investigators should give consideration to the MNV infection status of mice intended for these studies.

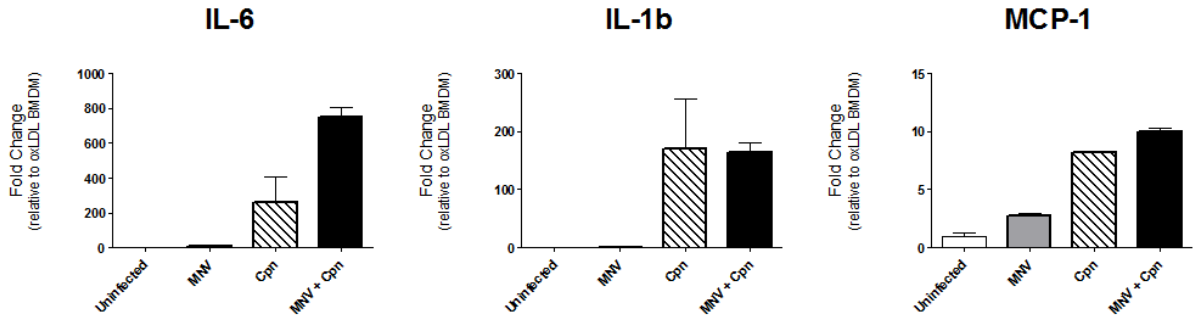

Figure 1: Fold change in IL-6, IL-1β and MCP-1 gene expression of oxidized LDL exposed ApoE$^{-/-}$ bone marrow-derived macrophages (BMDM) relative to uninfected control cells. Bars are (mean ± SEM) of replicate BMDM samples.

A.

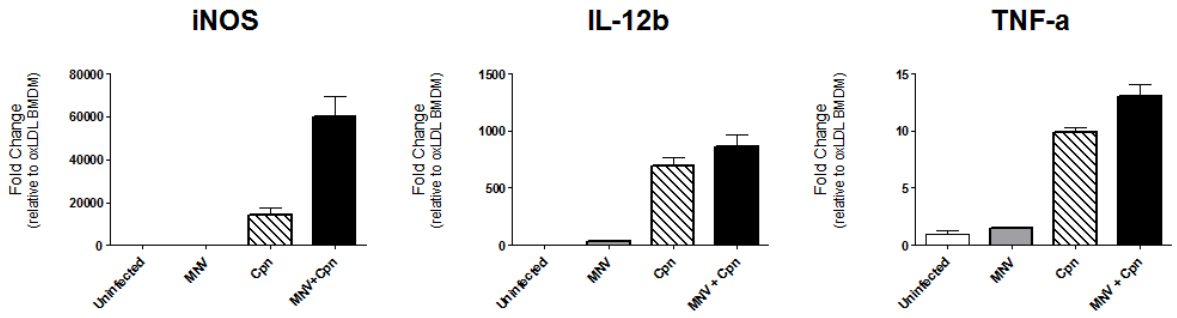

B.

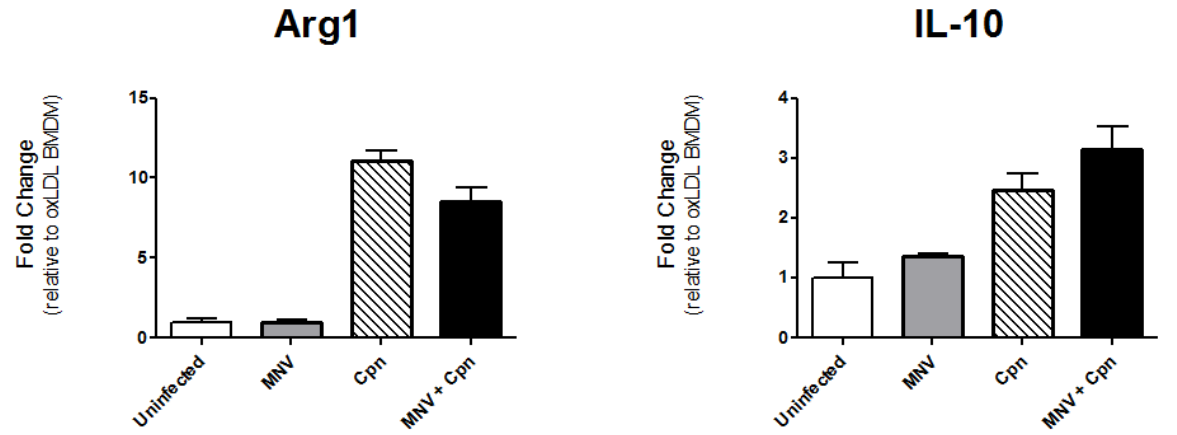

Figure 2: Fold change in gene expression of (A) iNos, Il-12β, and TNF-α (M1- associated genes) and (B) Arg1 and IL-10 (M2- associated genes) of oxLDL exposed ApoE$^{-/-}$ BMDM relative to uninfected control cells. Bars are (mean ± SEM) of replicate BMDM samples.

A.

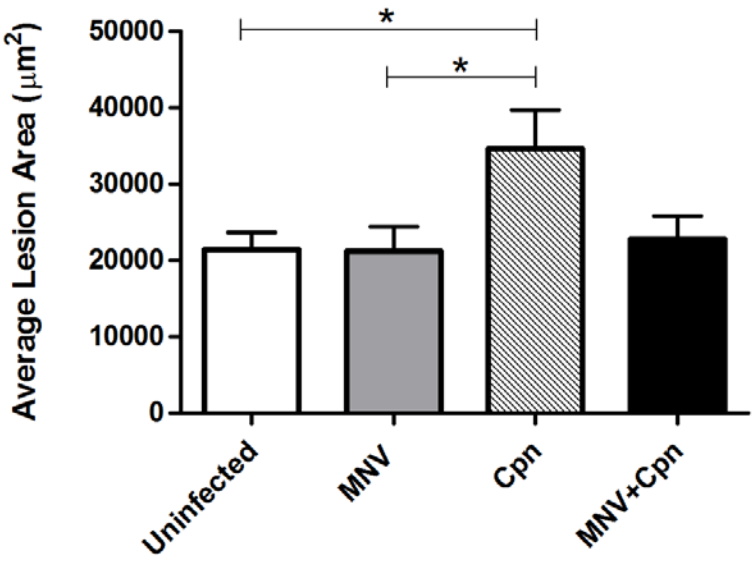

B.

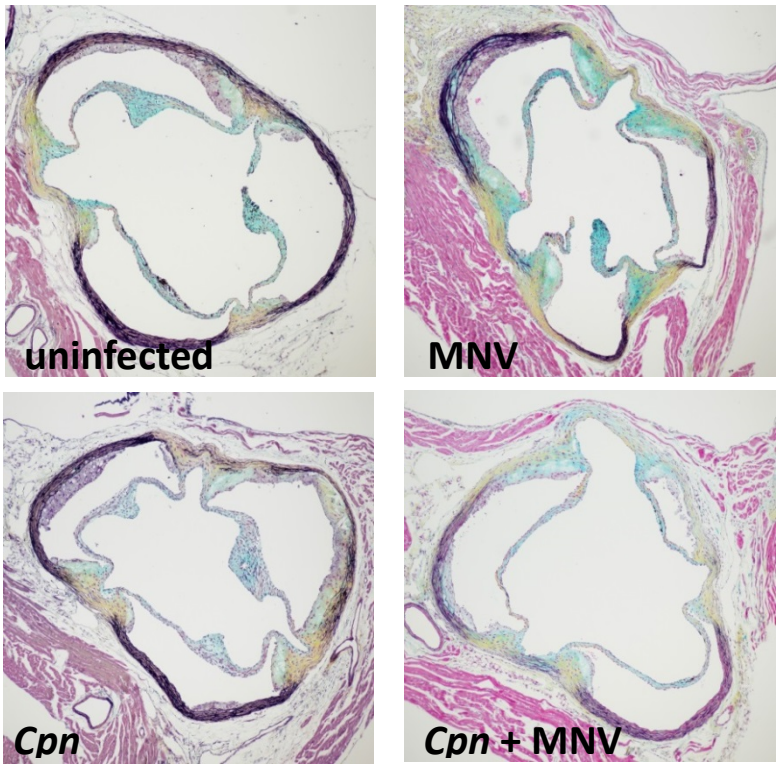

Figure 3: Aortic sinus lesion area was evaluated using Movat's pentachrome staining on serial sections of ApoE$^{-/-}$ mice. (A) Lesion area was determined by using computer-assisted morphometry n = 16-20 mice per infection group. (B) Representative lesions from mice of different infection status at endpoint, 8 weeks post MNV infection (20 weeks old). Magnification, 100×.

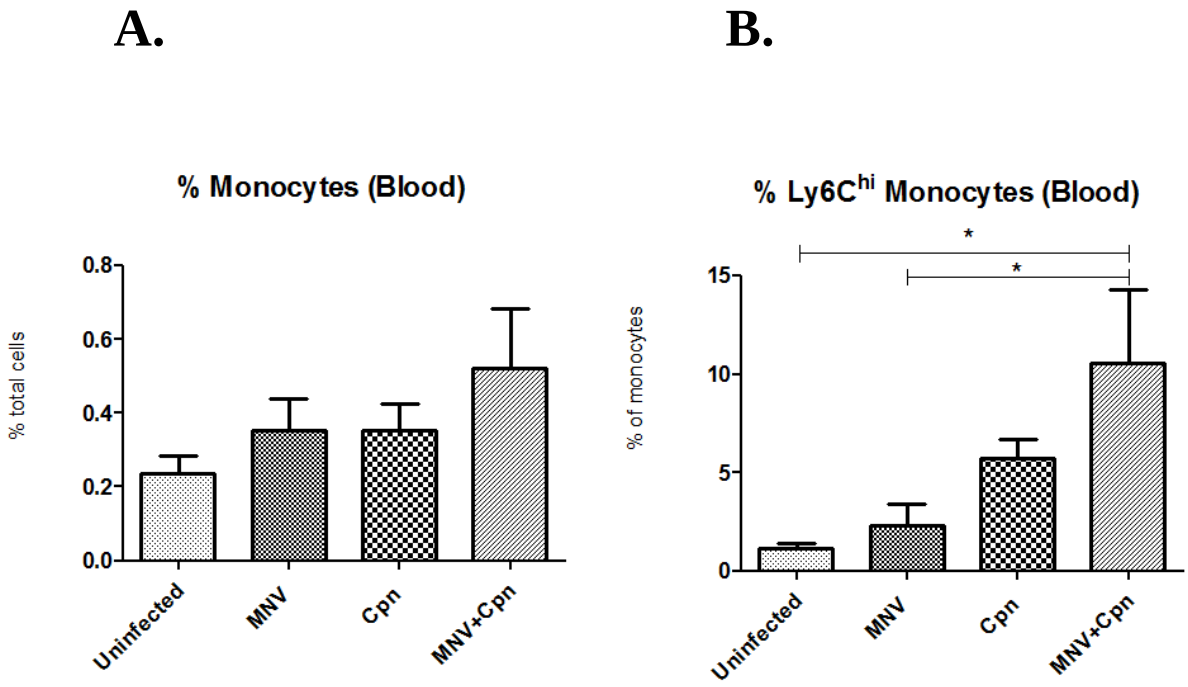

Figure 4: (A) Percentage of monocytes of total cells recovered from peripheral blood of 13-week-old ApoE-/- mice of various infection status and (B) percentage of Ly6C^{hi} monocytes of total monocytes. Samples with < 80 events in the monocyte gate were eliminated from analysis. n = 6-9 mice per infection group.

A.

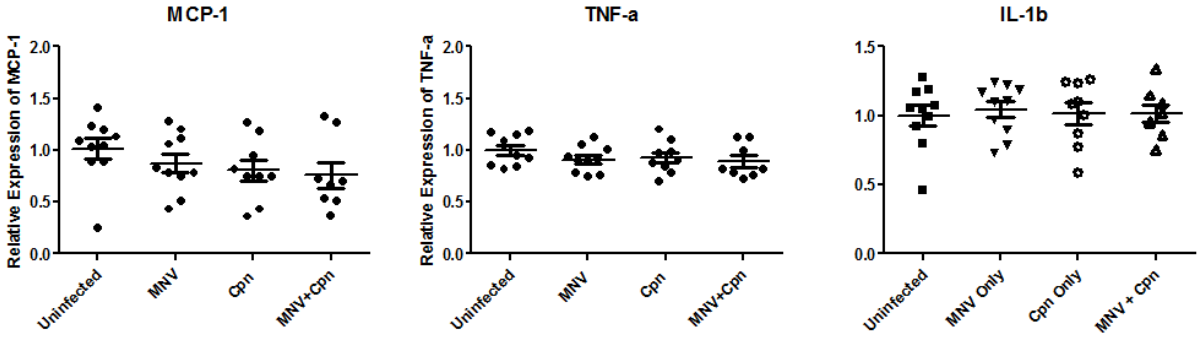

B.

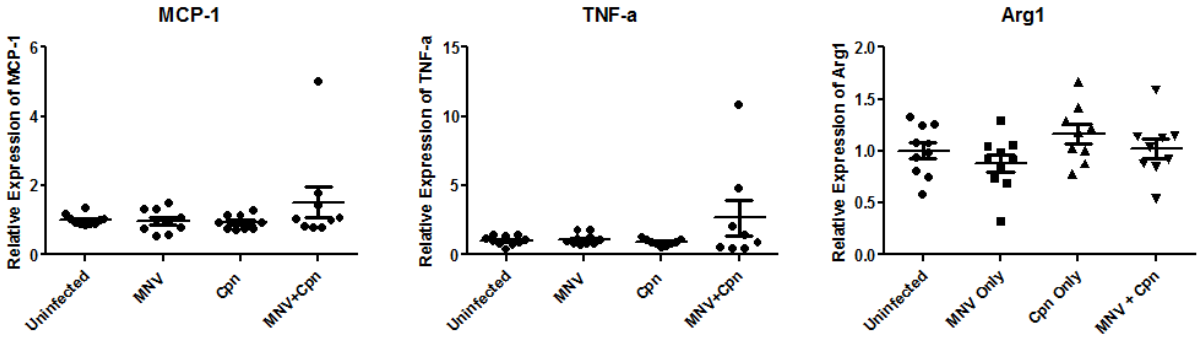

Figure 5: Relative expression of (A) MCP-1, TNF-α, and IL-1β in the aortic arch and (B) MCP-1, TNF-α, and Arg1 in unelicited peritoneal macrophages of 13-week-old ApoE-/- mice of various infection status. No significant differences were detected.

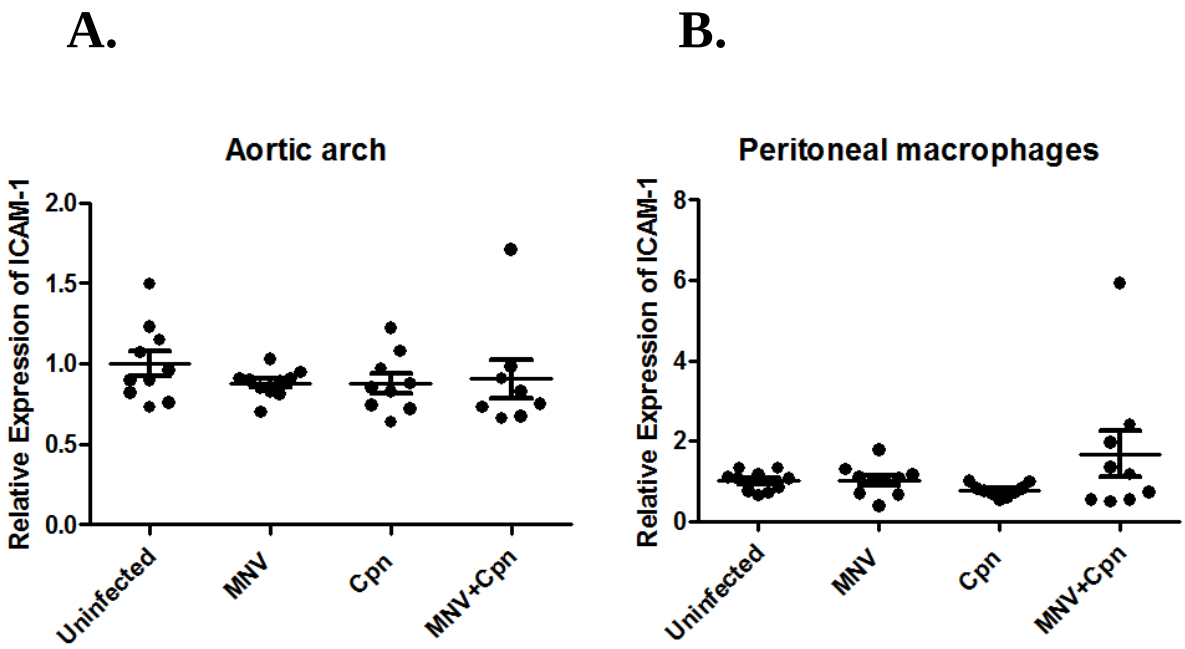

Figure 6: Relative expression of ICAM-1 in the (A) aortic arch and (B) unelicited peritoneal macrophages of 13-week-old ApoE-/- mice of various infection status. No significant differences were detected.

References

1. Blessing E, Campbell LA , Rosenfeld ME, Chough N, Kuo CC. 2001. *Chlamydia pneumoniae* infection accelerates hyperlipidemia induced atherosclerotic lesion development in C57BL/6J mice. Atherosclerosis, 158: 13–7.

2. Burnett MS, Gaydos C, Madico GE, Glad SM, Paigen B, Quinn TC, Epstein SE. 2001. Atherosclerosis in apoE knockout mice infected with multiple pathogens. J Infectious Diseases, **183**:226–231.

3. Burnett MS, Durrani S, Stabile E, Saji M, Lee CW, Kinnaird TD, Epstein SE. 2004. Murine cytomegalovirus infection increases aortic expression of pro-atherosclerotic genes. Circulation **109**: 893–897.

4. Cadwell K. 2015. Expanding the Role of the Virome : Commensalism in the Gut. **89**: 1951–1953.

5. Campbell LA, Moazed TC, Kuo CC, Grayston JT. 1998. Preclinical models for *Chlamydia pneumoniae* and cardiovascular disease: hypercholesterolemic mice. Clinical Microbial Infection **4**: 23–32.

6. Campbell LA, Kuo CC. 2004. *Chlamydia pneumonia* - an infectious risk factor for atherosclerosis? Nature Reviews Microbiology **2**: 23–32.

7. Chesebro BB, Blessing E, Kuo CC, Rosenfeld ME, Puolakkainen M, Campbell LA. 2003. Nitric oxide synthase plays a role in *Chlamydia pneumoniae*-induced atherosclerosis. Cardiovascular Research **60**: 170–174.

8. Duerkop BA, Hooper LV. 2013. Resident viruses and their interactions with the immune system. Nature Immunology **14**: 654–659.

9. Gracey E, Lin A, Akram A, Chiu B, Inman RD. 2013. Intracellular survival and persistence of *Chlamydia muridarum* is determined by macrophage polarization. PloS One, **8**: e69421.

10. Gui T, Shimokado A, Sun Y, Akasaka T, Muragaki Y. 2012. Diverse roles of macrophages in atherosclerosis: from inflammatory biology to biomarker discovery. Mediators of Inflammation e693083.

11. Hansson GK. 2005. Inflammation, atherosclerosis, and coronary artery disease. NEMJ **352**: 1685-1695.

12. Hayes EM, Tsaousi A, Gregoli KD, Jenkinson SR, Bond AR, Johnson JL, Newby AC. 2014. Classical and alternative activation and metalloproteinase expression occurs in foam cell macrophages in male and female ApoE null mice in the absence of T and B lymphocytes. Frontiers in Immunology **5**: e537.

13. Henderson KS. 2008. Murine norovirus, a recently discovered and highly prevalent viral agent of mice. Lab Animal **37**: 314–320.

14. Henkel JS, Beers DR, Siklós L, Appel SH. 2006. The chemokine MCP-1 and the dendritic and myeloid cells it attracts are increased in the mSOD1 mouse model of ALS. Molecular Cellular Neuroscience **31**: 427–437.

15. Herrera VL, Shen L, Lopez LV, Didishvili T, Zhang Y, Ruiz-Opazo N. 2003. *Chlamydia pneumoniae* Accelerates Coronary Artery Disease Progression in Transgenic Hyperlipidemia-Genetic Hypertension Rat Model. Molecular Medicine **9**: 135–142.

16. Hsich E, Fu Y, Paigen B, Johnson TM, Susan M, Epstein SE. 2001. Cytomegalovirus infection increases development of atherosclerosis in Apolipoprotein-E knockout mice. Atherosclerosis **156**: 23–28.

17. Hsu CC, Paik J, Brabb T, O'Brien KD, Kim J, Sullivan B, Hudkins K, Seamons A, Finley J, Meeker SM, Maggio-Price L. Murine norovirus infection variably alters atherosclerosis in apolipoprotein-E deficient mice. Comp Med [in press]

18. Hsu CC, Paik J, Treuting PM, Seamons A, Meeker SM, Brabb TL, Maggio-Price L. 2014. Infection with Murine Norovirus 4 Does Not Alter *Helicobacter*-Induced Inflammatory Bowel Disease in $Il10^{-/-}$ Mice. Comp Med **64**: 256–263.

19. Jupelli M, Shimada K, Chiba N, Slepenkin A, Alsabeh R, Jones HD, Crother TR. 2013. *Chlamydia pneumoniae* infection in mice induces chronic lung inflammation, iBALT formation, and fibrosis. PloS One **8**:e77447.

20. Kernbauer E, Ding Y, Cadwell K. 2014. An enteric virus can replace the beneficial function of commensal bacteria. Nature **516:** 94–98.

21. Khallou-Laschet J, Varthaman A, Fornasa G, Compain C, Gaston AT, Clement M, Caligiuri G. 2010. Macrophage plasticity in experimental atherosclerosis. PLoS One **5:** e8852.

22. Khan S, Rahman HNA, Okamoto T, Matsunaga T, Fujiwara Y, Sawa T, Akaike T. 2014. Promotion of atherosclerosis by *Helicobacter cinaedi* infection that involves macrophage-driven proinflammatory responses. Scientific Reports **4:** e4680.

23. Kuo CC, Shor A, Campbell LA, Fukushi H, Patton DL, Grayston JT. 1993. Demonstration of *Chlamydia pneumoniae* in Atherosclerotic Lesions of Coronary Arteries. J Infectious Diseases **167**: 841–849.

24. Leitinger N, Schulman IG. 2013. Phenotypic polarization of macrophages in atherosclerosis. ATVB **33**: 1120–1126.

25. Lencioni, KC, Seamons A, Treuting PM, Maggio-Price L, Brabb T. 2008. Murine norovirus: an intercurrent variable in a mouse model of bacteria-induced inflammatory bowel disease. Comp Med **58**: 522–33.

26. Lencioni KC, Drivdahl R, Seamons A, Treuting PM, Brabb T, Maggio-Price L. 2011. Lack of effect of murine norovirus infection on a mouse model of bacteria-induced colon cancer. Comp Med **61**: 219–226.

27. Lumeng CN, Bodzin JL, Saltiel AR. 2007. Obesity induces a phenotypic switch in adipose tissue macrophage polarization. J Clin Inv **117**: 175–184.

28. Madjid M, Awan I, Ali M, Frazier L. 2005. Influenza and atherosclerosis : vaccination for cardiovascular disease prevention. Ex Op Biotherapy **5**: 91–96.

29. Meeker S, Seamons A, Paik J, Treuting PM, Brabb T. Grady WM, Maggio-Price L. 2014. Increased dietary vitamin D suppresses MAPK signaling, colitis, and colon cancer. Cancer Research **74**:4398–4408.

30. Moazed TC, Campbell LA, Rosenfeld ME, Grayston JT, Kuo CC. 1999. *Chlamydia pneumoniae* infection accelerates the progression of atherosclerosis in apolipoprotein E-deficient mice. The J Infectious Diseases **180**: 238–241.

31. Nieto FJ. 1999. Viruses and atherosclerosis : A critical review of the epidemiologic evidence. A Heart J **138**: 453–460.

32. Paik J, Kwok F, Seamons A, Brabb T, Kim J, Sullivan B, Maggio-Price L. 2015. Effects of Murine Norovirus on Atherosclerosis in $Ldlr^{-/-}$ Mice Depends on the Timing of Infection. **65**: 114–122.

33. Paik J, Fierce Y, Drivdahl R, Treuting PM, Seamons A, Brabb T, Maggio-Price L. 2010. Effects of Murine Norovirus Infection on a Mouse Model of Diet-Induced Obesity and Insulin Resistance. **60:** 189–195.

34. Paik J, Fierce Y, Mai P, Phelps SR, McDonald T, Treuting P, Maggio-Price L. 2011. Murine norovirus increases atherosclerotic lesion size and macrophages in $Ldlr^{-/-}$ mice. Comp Med **61**:330–338.

35. Pritchett-Corning KR, Cosentino J, Clifford CB. 2009. Contemporary prevalence of infectious agents in laboratory mice and rats. Lab Animal **43**: 165–173.

36. Rosenfeld ME, Campbell LA. 2011. Pathogens and atherosclerosis: update on the potential contribution of multiple infectious organisms to the pathogenesis of atherosclerosis. Thrombosis and Hemostasis **106**: 858–67.

37. Sessa R, Pietro MD, Filardo S, Turriziani O. 2014. Infectious burden and atherosclerosis: A clinical issue. W J Clinical Cases **2**: 240-249.

38. Swirski FK, Weissleder R, Pittet MJ. 2009. Heterogeneous in vivo behavior of monocyte subsets in atherosclerosis. ATVB **29**: 1424–1432.

39. Swirski FK, Libby P, Aikawa E, Alcaide P, Luscinskas FW, Weissleder R, Pittet MJ. 2007. Ly-6C^{hi} monocytes dominate hypercholesterolemia-associated monocytosis and give rise to macrophages in atheromata. J Clinl Inv **117**: 195–205.

40. Swirski FK, Pittet MJ, Kircher MF, Aikawa E, Jaffer FA, Libby P, Weissleder R. 2006. Monocyte accumulation in mouse atherogenesis is progressive and proportional to extent of disease. PNAS **103**: 10340–10345.

41. Ward JM, Wobus CE, Thackray LB, Erexson CR, Faucette LJ, Belliot G, Green KY. 2006. Pathology of immunodeficient mice with naturally occurring murine norovirus infection. Tox Path **34**:708–715.

42. WHO. 2014. Global Status Report on Non-Communicable Diseases 2014.

43. Wobus, CE, Karst SM, Thackray LB, Chang K, Sosnovtsev SV, Belliot G, Virgin HW. 2004. Replication of Norovirus in cell culture reveals a tropism for dendritic cells and macrophages. PLoS Bio **2**: 2076–2084.

44. Zhu J, Quyyumi A, Norman JE, Csako G, Waclawiw M, Shearer GM, Epstein SE. 2000. Effects of total pathogen burden on coronary artery disease risk and C-reactive protein levels. A J Cardio **85:** 140–146.